Chiara Fania[1,2]
Luigi Anastasia[3,4]
Michele Vasso[1,5]
Nadia Papini[3,4]
Daniele Capitanio[1,2]
Bruno Venerando[3,4]
Cecilia Gelfi[1,2]

[1]Department of Sciences and Biomedical Technologies, University of Milan, Segrate, Milan, Italy
[2]Institute of Molecular Bioimaging and Physiology, National Research Council, Segrate, Milan, Italy
[3]Department of Medical Chemistry, Biochemistry and Biotechnology, University of Milan, Segrate, Milan, Italy
[4]Laboratory of Stem Cells for Tissue Engineering IRCCS Policlinico San Donato, San Donato, Milan, Italy
[5]LATO-HSR Giglio, Cefalù, Palermo, Italy

Received December 4, 2008
Revised March 25, 2009
Accepted March 26, 2009

Research Article

Proteomic signature of reversine-treated murine fibroblasts by 2-D difference gel electrophoresis and MS: Possible associations with cell signalling networks

Recent advances in stem cell biology have demonstrated that terminally differentiated adult cells can be induced to de-differentiate into progenitor cells (induced stem cells) upon proper stimuli. This has been achieved by the induced expression of key regulatory genes by retro- or lenti-viral systems. On the other hand, synthetic "small molecules" can also induce de-differentiation and may represent a potentially safer approach as compared with genetic manipulation. Along this line, a synthetic purine called "reversine" has been shown to induce the de-differentiation of fibroblasts into mesenchymal stem-cell-like progenitors, which can be successively induced to differentiate into skeletal muscle, smooth muscle and bone cells. The mechanism whereby reversine is able to achieve de-differentiation has yet to be clarified. In this context, we defined the protein changes induced by reversine treatment in murine fibroblasts by 2-D difference gel electrophoresis, coupled with MS. Proteins involved in cytoskeletal and cell shape remodeling, RNA export, degradation, folding, stress control and ATP production were found to be remarkably changed after reversine treatment. Ingenuity pathway analysis (IPA) predicted that these protein pattern changes enabled to propose that about 40 proteins might be associated to several biological functional networks, including cellular assembly, cell signaling and cell death. Altogether our data confirm the intrinsic complexity of the de-differentiation process induced by reversine and suggest more selected approaches to investigate the action mechanism of this small molecule.

Keywords:
2-D Difference gel electrophoresis / Fibroblasts / MS / reversine
DOI 10.1002/elps.200800800

1 Introduction

Over the past few years, a new discovery has generated wider perspectives in stem cell research. In fact, it was shown that terminally differentiated fibroblasts can be re-programmed into progenitor cells, almost indistinguishable from *bona fide* embryonic stem cells, as they possess almost identical gene expression profiles and exhibit analogous differentiation potential, including teratoma formation capability. In particular, S. Yamanaka's group found that the over-expression of four transcription factors (Oct 3/4, Sox2, c-Myc and Klf4) is able to reprogram somatic cells, namely skin fibroblasts, into embryonic-like stem cells, which were called *induced pluripotent stem* cells [1]. These findings generated great interest in the scientific community although the manipulation of the cell genome with the use of retro- or lenti-viruses rose some concerns about the safety of this experimental approach. In parallel, small molecules were also shown to be able to induce the de-differentiation process [2]. A synthetic purine, called "reversine", has been shown to induce the de-differentiation of myoblasts into mesenchymal progenitors [3], and reversine-treated human or murine fibroblasts could be induced to differentiate into skeletal muscle, smooth muscle and bone [4]. Thus, it might be envisioned that the use of small molecules (such as reversine) to increase cellular plasticity (that is to prompt terminally differentiated cells, such as fibroblasts, to trans-differentiate into different cell types) could be a possibly safer alternative to the *genetic*

Correspondence: Professor Cecilia Gelfi, Department of Sciences and Biomedical Technologies, University of Milan, L.I.T.A., Via Fratelli Cervi 93, 20090 Segrate, Milan, Italy
E-mail: cecilia.gelfi@unimi.it
Fax: +39-02-21717558

Abbreviations: DIGE, difference gel electrophoresis; **IPA**, ingenuity pathway analysis; **NL**, non-linear; **NPM**, nucleophosmin

manipulation approach, and would also provide an additional tool for investigating the complex mechanisms regulating cell differentiation. Along this line, an initial study on reversine mechanism of action showed that the molecule inhibits non-muscle myosin II heavy chain, and MAP kinase and that both activities are required for reversine effect [5]. Moreover, it was reported that some polycomb genes, which are normally involved in chromatin-based gene silencing, are activated by reversine [6]. These and other evidence [7–11] support the preliminary notion that reversine induces an initial growth arrest, which seems to be a key step for the reprogramming process. In order to fully consolidate this hypothesis, it will be of interest to define the protein pattern involved in growth arrest induction. A previous proteomic investigation on the effects of reversine on C2C12 (an immortalized carcinogenic cell line) based on conventional 2-DE on a pH 4–7 gradient, indicated a change in 32 protein spots, 22 of them identified [6]. The analysis revealed a differential expression of proteins involved in cell cycle control, protein biosynthesis and metabolism, cytoskeletal rearrangement, proteasome activity and electron transport. Based on these, a proteomic analysis on primary cultures of dermal fibroblasts, which represent a more attractive cell source as compared with C2C12, seems very appropriate, also in view of their potential therapeutic application. The aim of the present study was to define changes in protein expression induced by reversine treatment in primary cultures of murine fibroblasts using a more advanced analytical technology that is the 2-D difference gel electrophoresis (DIGE) coupled with MS. This technology allows a precise detection of minor differences of protein expression across multiple samples simultaneously with statistical confidence by using DeCyder software [12–14]. The presence of an internal standard, containing an aliquot of each sample under analysis, allows sample normalization. In addition, the linearity of the abundance changes, over four orders of magnitude, and the reproducibility of the method provide more reliable results than conventional approaches based on the comparison of the brightness of gel images obtained by conventional staining [15–19]. Proteins involved in cytoskeletal and cell shape remodeling, RNA export, degradation machinery, folding, stress control and ATP production were found to be changed after 4 days of 5 μM reversine treatment. Ingenuity pathway analysis (IPA) enabled to predict possible associations of these protein changes with some key biological networks.

2 Materials and methods

2.1 Cell culture and treatment

Primary mouse dermal fibroblasts were obtained from transgenic mice expressing green fluorescent protein [4]. They were cultured in DMEM high glucose, supplemented with 4 mM glutamine, 100 IU/mL penicillin, 100 μg/mL streptomycin and 10% v/v FBS. Cultures were performed at 37°C in a humidified incubator with 5% CO_2 and 95% air.

2.2 Treatment of fibroblasts with reversine

Reversine was prepared according to the published procedure [3] and purity (>98%) was checked by HPLC and LC-MS analysis. Mouse fibroblasts ($8–10 \times 10^4$) were plated in 100 mm dishes in DMEM supplemented with 10% FBS. Fibroblasts were treated with reversine, dissolved in DMSO, at concentration of 5 μM in 10% FBS DMEM, 18–24 h after seeding. Control cells were incubated with 0.05% DMSO. Treatment was carried out for 4 days without growth medium changes.

2.3 Cell cycle analysis

Control and treated cells were harvested and fixed in 70% ethanol and kept at 4°C before staining. Fixed cells were resuspended in 1 mL of a solution containing 5 μg/mL propidium iodide (Sigma) in PBS (Gibco Brl), 25 μL RNAse (Sigma) 1 mg/mL, 25 μL of Nonidet P40 (Sigma) 0.15% in water, and stained overnight at 4°C in the dark. Cell analysis was performed on at least 20 000 events for each sample by FACSCalibur System (BD) and DNA prole was analyzed by MODFit 3.0 (Verity Software House).

2.4 Protein extraction

Cultured reversine-treated and un-treated cells were washed twice with PBS and harvested in ice-cold PBS by scraping. After centrifugation at 800 × g for 10 min at 4°C the pellet was suspended in lysis buffer (7 M urea, 2 M thiourea, 4% CHAPS, 30 mM tris and 1 mM PMSF) and 0.1 mM PMSF and solubilized by sonication on ice. Proteins were selectively precipitated using PlusOne 2-D-Clean up kit (GE Healthcare) in order to remove non-protein impurities from samples, and re-suspended in lysis buffer. Protein extracts were adjusted to pH 8.5 by addition of 1 M NaOH. Protein concentration was determined with PlusOne 2-D-Quant kit (GE Healthcare).

2.5 Protein labelling and experimental design

Protein extracts (50 μg) from each set type of three separated culture plates, were labelled with 400 pmol Cy5 dye (CyDyes, GE Healthcare), whereas the internal standard, generated by pooling together an aliquot of each reversine-treated fibroblasts extracts and each control, was labelled with Cy3 dye (CyDyes, GE Healthcare). The minimal labelling was performed according to manufacturer's recommendations by incubating samples on ice in the dark for 30 min. The labelling reaction was quenched with 1 μL L-lysine 10 mM on ice for 10 min in the dark. The "two dyes" protocol was adopted. This experimental design was performed by acquiring the images with a two-laser scanner (Typhoon 9200, GE Healthcare) and utilizing the combina-

tion of Cy3:Cy5, due to their labelling efficiency and reliability compared with other dye combination, as described previously [12–15].

No preferential protein labelling or background noise were observed, but a larger gel number was required compared with the three dyes protocol. By utilizing the two dyes combination and the manufacturer's dye/protein ratio, no dye swap was needed since all samples that undergo the statistical analysis were labelled with the same dye (Cy5) and normalized against the same internal standard (labelled with Cy3).

2.6 2-D DIGE

Before IEF, labelled samples were diluted in an equal volume of 2× sample buffer containing 130 mM DTT and 2% v/v IPG buffer (GE Healthcare). Individual samples (40 μg) were combined with an equal amount of internal standard; rehydration buffer (7 M urea, 2 M thiourea, 2% CHAPS, 65 mM DTT, 0.5% IPG buffer pH 3.5–9.5 and BBF in traces) was added to a final volume of 450 μL. Samples were separated on 24 cm, pH 3–10 non-linear (NL) gradient IPGstrips (GE Healthcare), applying the following multi-step IEF protocol: 200 V (2 h), 500 V (2 h), 1000 V (2 h), 2000 V (1 h), 3000 V (1 h) and 8000 V until a total of 64 000 Vh was reached, using an IPGphor electrophoresis unit (GE Healthcare). Protein extracts from each sample were run in duplicate. After focusing IPGstrips were equilibrated in an SDS-reducing buffer (6 M urea, 2% SDS, 20% glycerol, 375 mM Tris-HCl, pH 8.8, 65 mM DTT) for 15 min, then alkylated for 8 min in the same buffer containing 135 mM iodoacetamide instead of DTT. Second dimension was carried out in 20 × 25 cm, 12%T, 2.5%C, over the total of monomers, constant concentration poly-acrylamide gels at 20°C and 15 mA *per* gel using the Ettan Dalt II system (GE Healthcare).

2.7 Image acquisition and analysis

CyDye-labelled gels were visualized using a Typhoon 9200 laser scanner (GE Healthcare). Excitation and emission wavelengths were chosen according to manufacturer's recommendations (532 and 633 nm laser beams; 580 and 670 nm emission filters). Spot detection was performed using DeCyder DIA module V. 6.5 (difference in-gel analysis, GE Healthcare). Inter-gel matching and statistical analysis were performed using a DeCyder BVA module V. 6.5 (biological variance analysis, GE Healthcare). For each gel undergoing the co-detection procedure, the estimated number of spots was set to 10 000, filters parameters were set as follows: slope >1.2, minimal area cut-off <250 and peak height <14. Statistically significant differences were computed by Student's *t*-test, the significance level was set at $p<0.01$. False discovery rate was applied as multiple test correction in order to keep the overall error rate as lower as possible. Only proteins with spot volumes consistently different in all replicates were considered differentially expressed.

2.8 Protein identification by MALDI-TOF and ESI-MS

For protein identification, in order to provide a proper amount of peptides for MS analysis, semi-preparative gels, containing 400 μg of total protein extract *per* strip, were loaded with unlabelled sample; electrophoretic conditions were the same as 2-D DIGE, except that gels were stained with a protein fluorescent stain, as recommended by manufacturer (Deep purple, 5 mL/L, GE Healthcare). Images acquisition was performed using Typhoon 9200 laser scanner. Spots of interest were excised from gel using the Ettan spot picker robotic system (GE Healthcare), destained in 50% methanol/50 mM ammonium bicarbonate and incubated with 30 μL of 4 ng/μL trypsin (Promega) dissolved in 10 mM ammonium bicarbonate for 16 h at 37°C. Released peptides were subjected to reverse phase chromatography (Zip-Tip C18 micro, Millipore), eluted with 50% acetonitrile/1% formic acid. An aliquot of 0.35 μL of peptides mixture was spotted onto the sample plate of an Ettan MALDI-TOF Pro (GE Healthcare) mass spectrometer; an equal volume of 10 mg/mL CHCA matrix dissolved in 70% acetonitrile/30% 50 mM citric acid was applied and spots were air dried at room temperature. MS proceeded at an accelerating voltage of 20 kV and spectra were externally calibrated using Peptide Mix 4 calibration mixture (Laserbio Labs); 256 laser shots were taken *per* spectrum. Proteins were identified by comparing the digest peaks with a computer-generated database of tryptic peptides from known proteins using the built-in search engine ProFound. Search was carried out by correlation of uninterpreted spectra to *Rodentia* entries in NCBInr database. For confirmation of identifications spectra were also searched against this database using MASCOT, which utilizes a robust probabilistic scoring algorithm. One missed cleavage *per* peptide was allowed and carbamidomethylation, as fixed modification, and methionine oxidation, as variable modification, were set. Peptide mass tolerance was set at 50 ppm. In cases where this approach was unsuccessful, additional searches were performed using ESI-MS/MS. MS/MS were recorded using a HCT Ultra mass spectrometer (Bruker Daltonics) interfaced to a MDLC capillary chromatograph (GE Healthcare). The samples were dissolved in 0.1% aqueous formic acid, injected onto a 0.075 × 150 mm Zorbax 300SB-C18 column (Agilent Technologies), and eluted with an acetonitrile/0.1% formic acid gradient. The capillary voltage was set to −1600 V, and data-dependent MS/MS acquisitions were performed on precursors with charge states of 2, 3 or 4 over a survey mass range of 300–1500. The collision gas was helium. Proteins were identified by correlation of uninterpreted MS/MS to *Mus musculus* entries in NCBInr, using MASCOT software. No mass and p*I* constraints were applied. One missed cleavage *per* peptide

was allowed, and the fragment ion tolerance window was set to 0.3 Da. Carbamidomethylation of cysteine was set as fixed modification, whereas methionine oxidation as variable modification. Where identification was based on a single matching peptide, the sequence was confirmed by DeNovo Sequencing (Biotools, Bruker Daltonics).

2.9 SDS Electrophoresis for HMW protein separation and quantitation

SDS electrophoresis was performed on controls and reversine-treated cellular extracts on a 37% glycerol, 6% polyacrilamide gel according to [20]. Samples (50 μg) were run in duplicate at 100 V, overnight. Gels were stained with SYPRO Orange (Molecular Probes) and scanned using a 570 nm emission filter on Typhoon 9200 laser scanner (GE Healthcare). Protein band quantification was achieved using Image Quant software (Molecular Dynamics). Molecular weight markers containing M1C from rabbit (212 kDa) and bovine α2-macroglobulin (170 kDa) were run in a separate lane. Differences between groups were computed by a two-tail *t*-test and setting the significativity level at $p < 0.05$. Proteins over 200 kDa, differentially expressed or not, were excised from gel and hydrolysed by trypsin, as previously described, after reduction and alkylation of cysteine residues by 10 mM DTT (100 μL, 45 min at 56°C) and 55 mM iodoacetamide (100 μL, 30 min at room temperature in the dark) respectively. Proteins were identified by ESI-MS/MS.

2.10 Immunofluorescence

Cells were washed with PBS, fixed with 4% w/v paraformaldehyde in PBS and permeabilized with 0.1% w/v Triton X-100 in PBS with 1% w/v bovine serum albumin for 30 min. Then, cells were incubated with goat polyclonal anti-lamin A/C antibody (Santa Cruz) (1:50 dilution) for 2 h at room temperature. After incubation cells were washed three times in PBS and incubated with the appropriate TRIC-conjugated secondary antibody (Sigma) for 1 h at room temperature. After washing in PBS, cells were analyzed under a fluorescence microscope (1 × 51 Olympus, equipped with an XCite Series 120 fluorescence apparatus, Hammamatsu C8484 digital camera and CellF Imaging Software). Images of reversine-treated and un-treated cells were acquired in the same experimental conditions (for TRITC, acquisition time 200 ms, gain is 1) to avoid possible artifacts. Moreover, a surface plot test was done with ImageJ software to compare the fluorescence signal acquired in the two images.

2.11 Immunoblotting

To correlate MALDI-TOF results with changes in p*I*s and apparent molecular mass provided by 2-D gels, annexins A3 were confirmed by immunoblotting. For that, a total of 100 μg of control and reversine-treated protein extracts were resolved by 2-D PAGE, transferred and blocked onto a PVDF membrane (300 mA; 180 min) utilizing a Transblot Cell from GE Healthcare. The membranes were blocked overnight in TBS (20 mM Tris, 137 mM NaCl, 0.1% Tween, pH 7.5) containing 2% Blocking Agent powder (GE Healthcare). Subsequently the membranes were incubated with monoclonal anti-annexin A3 (1:30 000 as primary antibody; Abnova) and HRP conjugate anti-mouse (1:70 000 as secondary antibody; GE Healthcare). Proteins were visualized by chemiluminescence using ECL Advance kit (GE Healthcare).

To investigate protein ubiquitination, a 2-D immunoblotting was performed with the use of a highly specific primary antibody. One hundred microgram of protein extract from control and reversine-treated fibroblasts respectively was resolved by 2-D PAGE as described previously and transferred onto PVDF membranes. Membranes were then incubated with antibodies diluted as follows: monoclonal anti-ubiquitin (1:20 000 as primary antibody, Cell Signaling Technology) and HRP conjugate anti-mouse (1:50 000 as secondary antibody, GE Healthcare). Proteins were visualized by chemiluminescence using ECL Advance kit (GE Healthcare).

2.12 Bioinformatic data analysis

Differentially expressed proteins were evaluated by IPA (Ingenuity System, Montain View, CA, USA). IPA is a software application that enables to identify the biological mechanisms, pathways and functions matching a particular dataset of proteins. IPA is based on a database obtained by abstracting and interconnecting a large fraction of the biomedical literature according to a very strict algorithm. This database integrates protein functions, cellular localization, small molecules and disease inter-relationships. The networks are displayed graphically as nodes, representing individual proteins and edges representing the biological relation between nodes. Networks are ordered by score and optimized including as many differentially expressed proteins as possible. A *p*-score (*i.e.* $-\log(p\text{-value})$) for each possible network is computed. Therefore, networks with scores of 2 or higher have at least 99% confidence of not being generated by random chance alone.

3 Results and discussion

A number of molecules and genes have been already defined as targets of reversine. However, a precise mechanism of the reversine-mediated de-differentiation process has yet to be disclosed. Therefore, a proteomic approach could represent an essential tool to provide better insights into reversine's mode of action. Proteomic analyses were carried out on approximately 1×10^7 reversine-treated and control murine fibroblasts, isolated

from transgenic mice expressing green fluorescent protein. Fibroblasts were grown for 4 days in the presence of 5 μM reversine in growth medium as described by Anastasia *et al.* [4]. Control cells were treated with the same volume of DMSO, which was used to dissolve reversine. Treatment efficacy was assessed by cell cycle analysis and flow cytofluorimetry. The results indicated the formation of a tetraploid cell population already after 3 h in treated cells, reaching about 90% at the end of the treatment, as shown in Fig. 1. In addition, 20% of treated fibroblasts shifted from a diploid/mononuclear (2n) to a tetraploid/binuclear ($2 \times 2n$) population, confirming previous observations [3].

To assess changes of the protein pattern due to the reversine treatment, proteins from cell extracts were separated by a 2-D DIGE methodology, utilizing a 24 cm, pH 3–10 NL gradient as first dimension. This method labels proteins with fluorescent dyes before 2-DE, enabling accurate analysis of differences in protein abundance between samples. A representative 2-D map of the obtained fibroblast proteome is shown in Fig. 2. Overall, approximately 2700 spots were matched *per* gel, and 75 were differentially expressed (*t*-test, $p < 0.01$) in treated *versus* untreated cells. The protein load increment, which is necessary for MS identification, induces a loss of isoforms resolution and a consequent minor number of represented spots [21]. Thus, only 66 of the differentially expressed spots were picked up and 53 of them identified by MALDI-TOF and ESI-MS/MS. Some of the differentially changed spots were very faint and close to the limit of 2-DDIGE, consequently, after gel excision and digestion, these spots were below the sensitivity of our mass instruments and remained undetectable. Identified spots are indicated and numbered in Fig. 2. For each spot the statistical analysis (average ratio and *p*-values), the identification parameters and protein accession numbers, together with the molecular mass and p*I*, are listed in Table 1. Detailed MS data are listed in Table 1S as Supporting Information. Average ratios for each differentially expressed protein isoforms are also reported later on in the text to facilitate the possible biological interpretation.

3.1 Semi-quantitation of the high-molecular-weight proteins by SDS electrophoresis

Figure 3 shows qualitative results on high-molecular-weight proteins (over 200 kDa), which could not be detected by 2-DE analysis, by SDS electrophoresis as described in Section 2. Differential analysis, conducted by Image Quant after Sypro Orange staining, indicated that only two bands over 200 kDa were differentially changed. The two bands over 200 kDa were excised, digested with trypsin and analyzed by ESI-MS/MS. ESI-MS/MS results are summarized in Table 2 and in Supporting Information Table 1S. Two ubiquitously expressed isoforms of Filamin, A and B, were significantly ($p < 0.05$) underexpressed in reversine-treated samples. Filamins are known to bind actin, different molecules and ions involved in the cellular signaling and transcriptional regulation [22–24]. In particular Meng *et al.* [25] suggested that filamin A plays a role in mechanisms making cells more vulnerable to several DNA-damaging agents and that lack of filamin A causes a delay in G2 recovery after irradiation.

Myosin II heavy chain isoforms were also identified. No changes in protein abundance were visualized ($p = 0.09$), confirming that reversine treatment does not induce an increment of non-contractile high-molecular-weight myosins II but its role is related to its ATPase activity inhibition [5]. To better clarify this issue further investigations will be required.

The results provided by this differential analysis support data from previous studies, confirming the effects of reversine on cell cycle, cell proliferation and cell morphology [4–6]. According to gene ontology the differentially expressed proteins were clustered into four major categories: cytoskeletal and cell shape, degradation machinery, stress control and metabolic proteins.

To gain better insights into biological significance of the quantitative differential results, differentially expressed proteins were analyzed by IPA Software (www.ingenuity.com). IPA is a software application that enables to identify

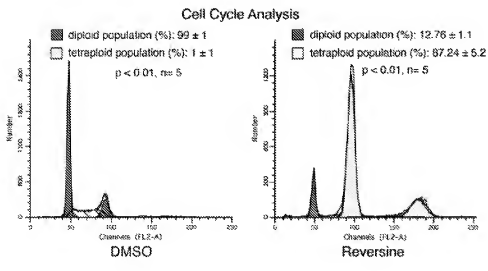

Figure 1. Effects of reversine treatment on fibroblasts cell cycle. Flow cytometry analysis on five samples performed after 72 h of DMSO (control) or 5 μM reversine treatment. After reversine treatment for 72 h, the percentage of diploid population was 12.76 +/− 1.1, whereas the percentage of tetraploid population was 87.24 +/− 5.2. In control samples the percentage of diploid/tetraploid population was 99 +/− 1 and 1 +/− 1, respectively.

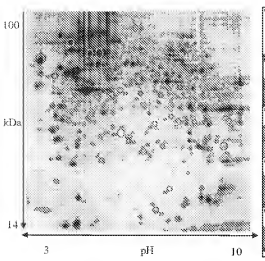

Figure 2. Representative 2-D DIGE map of fibroblast protein extract labelled with Cy3. Fifty micrograms of protein extract were separated in a NL pH 3–10 IPG strip in the first dimension and SDS gel (12% T, 2.5% C) in the second and acquired with a 532 nm laser beam and 580 nm emission filter. DeCyder software allowed to detect approximately 2700 spots. Differential analysis of reversine-treated fibroblast cells compared to control (statistical analysis was performed by BVA module of DeCyder) revealed 75 differentially expressed ($p<0.01$) protein spots. Identified proteins were indicated by circles and numbered as in Table 1. DeCyder Software 3-D views for differentially changed spots 2, 3, 4, 8 and 9 are also showed.

the biological mechanisms, pathways and functions matching a particular dataset of proteins. In this study 55 differently abundant proteins were uploaded utilizing IPA bioinformatic tool. Among them, 42 proteins were involved in networks on the basis of IPA criteria. As summarized in Table 3, IPA indicated a total of five networks with the following scores: 33 (16 molecules involved), 23 (12 molecules involved), 22 (12 molecules involved), 2 (1 molecule involved) and 2 (1 molecule involved), respectively. Two out of five networks (1 and 2) shown in Fig. 4A and B, respectively, appear to overlap. The networks with high score are associated with cellular assembly and organization, cancer, cell-to-cell signaling and interaction, cell death, neurological disease, molecular transport and cellular function and maintenance. In particular, proteins were grouped into functional categories based on their biochemical role.

3.2 Cytoskeletal and cell shape remodeling

Active remodeling of the cytoskeleton is fundamental to most biological processes that involve motility and changes in cell morphology, including cell migration, spreading, division and cell fusion. Changes in cell morphology can be elucidated by observing variations of proteins involved in actin filaments dynamics and remodeling [26]. Differential analysis showed a positive increment of cofilin 1 and Rho GDI α (+1.3- and +1.49-fold, respectively) in reversine-treated cells. Cofilin 1 promotes actin filament disassembly [27], which is present in myotubes and its phospho/dephosphorylation is essential for cytoskeletal rearrangement [28]. On the other hand, Rho GDI is an inhibitory regulator and promotes the reorganization of actin filaments with a consequent cytoskeletal remodeling [29]. Tropomyosin beta, which stabilizes actin in non-muscle cells, and Tropomodulin 3, which blocks elongation and depolymerization of actin filament, were also found increased (+1.54- and +1.67-fold, respectively).

Another strongly increased protein target of reversine action was β-tubulin (+1.66-fold), a cytoskeletal protein, which is highly abundant in microtubules [30] and that plays a crucial role in cytoskeletal remodeling. In particular, an increment of β-tubulin promotes the assembly and organization of the cytoskeleton into 3-D structures by binding the vinculin, moesin and the disassembly of actin depolymerizing factor/cofilin [31]. In treated protein extracts, vinculin (+1.33), and two subunits of moesin (+1.79- and +2.21-fold) were more abundant.

Rho GDI, cofilin and tropomyosin are known regulators of actin filament dynamics and membrane extensions. The increased levels of Rho GDI-α (+1.49) rely on the dynamic reorganization of the actin cytoskeleton, contributing to control membrane protrusions associated with apoptosis [32] and cell injury [33]. In addition, cofilin is essential for a rapid turnover of actin filaments, actin polymerization and membrane protrusions, and has the capacity to determine the direction of cell motility [34, 35]. By combining these results, we can speculate on a positive action of reversine in cytoskeletal reorganization, and on its negative modulation of the pro-apoptotic formation of protrusions on the cell surface.

In contrast to the increment of some cytoskeletal proteins, nucleophosmin (NPM) was decreased (−1.85-fold). This protein is also involved in cell-shape changes, as it is a highly phosphorylated protein associated with the nucleolar ribonucleoprotein structures, which were previously found decreased in reversine-treated cells [36]. NPM is involved in many cellular processes but its function remains unknown. Amin *et al.* [37] demonstrated that in HeLa cells, NPM causes distortion of nucleolar structure leading to a multiple micronuclei formation induced by a cytoskeletal rearrangement. Moreover a decrement of NPM produces reduced cellular proliferation and apoptosis [38].

A similar decrement (−1.78-fold) was also observed in a tumor protein, translationally controlled 1 (TPTC 1), an anti-apoptotic protein involved in calcium binding and microtubule stabilization [39].

Interestingly lamin C, which determines nuclear shape and size, was increased (+2.41-fold).

Physiologically the presence of lamin C is related to cellular differentiation [40]. It is known that nuclear lamin A/C deficiency induces defects in cell mechanics, polarization and migration. Actually, lamin A/C deficiency leads to nuclear fragility and cytoplasmic mechanical rigidity by reducing its elasticity and viscosity [41]. Moreover, lamin

Table 1. Differentially changed proteins in reversine-treated fibroblasts compared with control cells[a)]

Spot number	*t*-Test *p*-value	Average ratio V_R/V_C (fold-change)	Name	*pI*	Molecular weight (Da)	Swiss-Prot accession number	Method	MASCOT score	Identified peptides	Coverage (%)
1	0.0081	1.33	Vinculin	5.77	116 717.36	Q64727	MS/MS	731	26	26
2	0.009	1.79	Ubiquitin-activating enzyme E1, Chr X	5.43	117 808.94	Q02053	PMF	136	13	14
3	0.0065	1.74	Ubiquitin-activating enzyme E1, Chr X	5.43	117 808.94	Q02053	PMF	88	10	10
4	0.0037	−1.45	Tumour rejection antigen gp96	4.72	90 096.75	P08113	PMF	118	12	13
5	0.0024	1.79	Moesin	6.22	67 766.99	P26041	MS/MS	326	12	20
6	0.0077	2.21	Moesin	6.22	67 766.99	P26041	MS/MS	509	14	27
7	0.0094	2.41	Lamin C [*Mus musculus domesticus*]	6.54	74 237.57	P48678	PMF	214	22	41
8	0.0011	−1.47	Heat shock cognate 71 kDa protein	5.37	70 871.07	P63017	MS/MS	1230	25	46
9	0.0074	1.23	HSP9A	5.81	73 491.28	Q3TW93	PMF	71	8	16
10	0.0033	2.03	Phosphoenolpyruvate carboxykinase 2	6.92	70 527.9	Q8R3X7	PMF	73	8	14
11	0.0087	1.17	Calreticulin	4.33	47 994.52	B2MWM9	PMF	112	28	23
12	0.0026	−1.23	Chaperonin containing TCP-1 θ subunit	5.44	59 568.65	Q9WVS5	PMF	131	13	26
13	0.003	−1.68	Vacuolar adenosine triphosphatase subunit B	5.57	56 550.8	P62814	PMF	144	11	27
14	0.0034	1.41	Glutamate dehydrogenase 1, mitochondrial precursor	8.05	61 336.79	P26443	MS/MS	242	6	23
15	0.0028	1.63	Serine hydroxymethyltransferase 2 (mitochondrial)	8.73	55 758.73	Q9CZN7	MS/MS	556	16	32
16	0.0065	2.14	Cytochrome P450, family 19, subfamily a, polypeptide 1	8.22	58 015.17	P47738	PMF	76	7	13
17	0.0098	−1.45	DEAD (Asp-Glu-Ala-Asp) box polypeptide 39	5.46	49 067.40	Q8VDW0	MS/MS	276	9	24
18	0.0018	1.66	Tubulin β-5 chain	4.78	49 670.82	P99024	MS/MS	133	3	6
19	0.0017	1.66	47 kDa HSP	8.82	44 849.37	P19324	PMF	70	8	23
20	0.0043	1.63	Annexin A7	5.91	49 939.30	Q07076	MS/MS	63	2	5
21	0.0041	2.35	Acyl-coenzyme A thioesterase 2, mitochondrial precursor (Acyl-CoA thioesterase 2)	6.91	49 652.02	Q9QYR9	MS/MS	98	3	8
22	0.0087	1.79	Cathepsin D [Precursor]	6.49	42 940.33	P18242	MS/MS	97	1	8
23	0.0025	1.69	Long chain-specific acyl-CoA dehydrogenase, mitochondrial precursor	8.53	47 907.95	P51174	MS/MS	204	5	13
24	0.00085	−1.13	Selenophosphate synthetase 1	5.62	42 934.63	Q6P1B6	MS/MS	168	2	8
25	0.0093	3.55	Fructose-bisphosphate Aldolase	8.3	39 355.93	Q5FWB7	PMF	142	11	41
26	0.0021	1.63	NADH dehydrogenase (ubiquinone) 1 α subcomplex 10	7.63	40 603.43	Q99LC3	MS/MS	151	3	15
27	0.0062	1.39	Annexin A3	5.33	36 239.81	Q35639	PMF	144	11	32
28	0.0015	−1.85	Nucleophosmin 1	4.62	32 560.07	Q61937	MS/MS	95	1	5
29	0.0022	−1.16	Heterogeneous nuclear ribonucleoprotein A2/B1 isoform 2	8.97	37 402.67	Q88569	PMF	82	6	36
30	0.0022	−1.36	Annexin A3	5.33	36 239.81	Q35639	PMF	164	12	35
31	0.0033	1.13	Annexin A5	4.83	35 752.44	P48036	PMF	153	11	37
32	0.0038	2.7	Electron transfer flavoprotein subunit α, mitochondrial precursor (α-ETF)	8.62	35 009.44	Q99LC5	MS/MS	669	6	24
33	0.0042	3.96	Pyrroline-5-carboxylate reductase 1	6.36	32 373.41	Q922W5	PMF	107	9	34
34	0.0038	1.46	Annexin A5	4.83	35 752.44	P48036	PMF	96	9	27
35	0.0053	1.64	Mtr3 (mRNA transport regulator 3)-homolog	5.87	28 370.15	Q8BTW3	MS/MS	115	4	16
36	0.0023	1.25	Proteasome (Prosome, macropain) 28 subunit, α	5.73	28 672.94	Q5HZK3	MS/MS	62	1	10
37	0.0031	1.15	NG,NG-dimethylarginine dimethylaminohydrolase 2 (Dimethylargini-nase-2) (DDAHII) (DDAH-2)	5.66	29 645.83	Q99LD8	MS/MS	109	4	15
38	0.0043	1.31	Endoplasmic reticulum protein ERp29 precursor	5.90	28 823.25	P57759	PMF	70	6	27
39	0.0043	1.53	Enoyl-CoA hydratase1 protein, mithocondrial	8.76	31 474.37	Q8BH95	MS/MS	394	6	22
40	0.0017	1.49	Rho GDP dissociation inhibitor α	5.12	23 276.22	Q99PT1	MS/MS	146	2	16
41	0.00038	−1.54	Triosephosphate Isomerase	6.90	26 712.62	P17751	MS/MS	225	5	22
42	0.0096	−1.13	Proteasome (prosome, macropain) subunit, α type 6	6.35	27 372.43	Q9QUM9	PMF	80	6	28

Table 1. Cont.

Spot number	*t*-Test: *p*-value	Average ratio *Vv*/*Vc* (fold-change)	Name	p*I*	Molecular weight (Da)	Swiss-Prot accession number	Method	MASCOT score	Identified peptides	Coverage (%)
43	0.00692	2.07	Glutathione *S*-transferase, mu 1	8.14	25 838.8	P10649	PMF	72	5	22
44	0.0038	−1.61	Triosephosphate isomerase 1	6.90	26 712.62	P17751	MS/MS	1181	8	40
45	0.0019	2.69	Glutathione *S*-transferase, mu 2	7.31	25 585.51	P15626	MS/MS	128	2	12
46	0.0007	1.41	Peroxiredoxin 3	5.73	21 564.58	P20108	PMF	80	5	24
47	0.0051	−1.78	Tumor protein, translationally controlled 1	4.76	19 462.17	P63028	MS/MS	155	4	24
48	0.0045	1.58	Actin, beta, muscle	5.37	41 635.98	P60709	MS/MS	191	5	24
49	0.0046	1.3	Actin, alpha 1, skeletal	5.23	42 023.86	P68135	MS/MS	173	4	28
50	0.0091	−1.46	Ubiquitin-conjugating enzyme E2 variant 1	7.75	16 354.73	Q9CZY3	MS/MS	104	3	28
51	0.0013	1.41	Interleukin-25	5.94	15 741.61	Q9CRT4	MS/MS	73	1	11
52	0.0076	1.67	Tropomodulin 3	5.02	39 902.72	Q3UHJ0	MS/MS	285	7	21
53	0.0011	1.54	β-Tropomyosin	4.66	32 838.70	P58774	MS/MS	442	9	35

a) *Vv*/*Vc* indicates the value derived from the normalized spot volume standardized against the intra-gel standard provided by DeCyder software analysis.

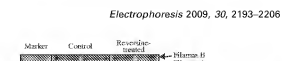

Figure 3. Qualitative SDS-PAGE of high-molecular-weight proteins from controls and reversine-treated fibroblast protein extracts. Fifty micrograms of protein extract were loaded *per* lane. Electrophoresis was carried out in a discontinuous buffer system with a 4% T stacking gel, pH 6.8 and a 6% T, 37% w/v glycerol, pH 8.8 running gel. Samples were separated overnight at 100 V. Gels were stained with SYPRO orange and scanned at 570 nm emission filter with a Typhoon laser scanner.

A/C deficiency induces significant separation of the microtubule organizing center from the nuclear envelope. Altogether these results show that both the physical properties of the cytoskeleton and the cytoskeleton-based processes, including cell motility and cell polarization, depend on the nuclear lamina. These findings suggest the existence of a functional mechanical connection between the nucleus and the cytoskeleton, which is influenced by reversine [42].

3.3 Protein degradation machinery

A significant differential expression was also found in proteins involved in protein degradation, such as ubiquitin-activating enzyme E1, ubiquitin-conjugating enzyme E2 variant 1, proteasome 28 subunit α, proteasome subunit α type 6, vacuolar adenosine triphosphatase subunit B and cathepsin D.

It is known that in eucariotic cells the degradation machinery can follow lysosome and/or proteasome pathways: both of them were shown here to be deregulated by reversine treatment. Proteasome 28 subunit α is a 249 amino acids small activator of a peptidase, activating hydrolysis of small non-ubiquitinated peptides by means of the 20S proteasome [43]. However, even if its precise cellular function remains only partially understood [44] we found its expression increased (+1.25). On the contrary, the Proteasome subunit α type 6 expression was slightly decreased (−1.13). This protein is one of the subunits constituting the 20S proteasome core, which is responsible for the hydrolitic activity. In particular, the α subunit represents one of the two outer rings whose function is to bind the 19S regulatory subunit, forming a channel essential for the degradation of denatured proteins [45]. The effects of proteasome inhibition on the stability of various cell cycle regulatory proteins are well established and include the arrest of mitogen-induced proliferation, inhibition of cell cycle entry and apoptosis [46, 47].

Together with slight changes on proteasome subunit assembly, a differential expression of two enzymes involved in the ubiquitination pathway, ubiquitin-activating enzyme E1 (+1.74-fold in spot 3 and +1.79-fold in spot 2) and ubiquitin-conjugating enzyme E2 variant 1 (−1.46-fold) was observed. The first enzyme plays a role in recruiting

Table 2. High-molecular-weight proteins identified by MS

Name	p*I*	Molecular weight (Da)	Swiss-Prot accession number	MASCOT Score	Identified peptides	Coverage (%)
Filamin-A	5.68	281 193.50	Q8BTM8	1789	71	38
Filamin-B	5.44	277 752.59	Q80X90	2133	70	39
Myosin, heavy polypeptide 9, non-muscle isoform 1	5.54	226 372.08	Q8VDD5	829	25	19

Table 3. The high-scored biological networks in murine reversine-treated fibroblast cells[a)]

Network ID	Genes in network	Top functions	Score	Focus molecules
1	**ACADL**, **ACOT2**, **ALDH2**, ATF4, **ATP6V1B2**, CDK2, CREB1, **CTSD**, EGF, **EXOSC6**, **GSTM1 (includes EG:2944)**, HNF4 alpha dimer, **HSP90B1**, HTT, IL4, IL6, IL12, KITLG (includes EG:4254), LY6E, NFE2L2, **NPM1 (includes EG:18148)**, **PCK2**, **PSMA6**, PSMB7, PSMB8, **PSME1**, PSME2, **PYCR1**, retinoic acid, RNF128, **SHMT2**, SWAP70, **TPT1 (includes EG:22070)**, **TUBB**	Cell-to-cell signaling and interaction, endocrine system development and function, molecular transport	33	16
2	**ANXA5**, **ARHGDIA**, ARHGEF1, **C190RF10**, **CFL1**, **DDAH2**, Erm, EZR, F Actin, F2RL1, FOS, Ige, LIMK2, LMNA, LY6E, MARCKSL1, MKL1, **MSN**, MYH7, PFN, PIP5K1B, RDX, retinoic acid, RHOA, Rock, TGFB1, **TMOD3**, TNNT2, **TPI1**, **TPM2**, Tropomyosin, TTN, **UBA1**, VASP, **VCL**	Cell morphology, cellular assembly and organization, cellular function and maintenance	23	12
3	**AK1**, **ALDOA**, **ANXA3**, **ANXA7**, BAG3, Ca2+, CCT2, CCT3, CCT4, CCT5, CCT7, **CCT8**, CCT6A, COL3A1, DNAJ, DNAJC13, **ERP29**, **GLUD1**, **GSTM1 (includes EG:14862)**, **HSPA8**, **HSPA9**, IGF1R, INS1, KCNJ11, KLF4, L-glutamic acid, **SERPINH1**, SRI, ST13, STIP1, TCP1, TDP1, TP53, **UBE2V1**, VHL	Cancer, cell death, neurological Disease	22	12
4	**ETFA**, HEXB	Carbohydrate metabolism, lipid metabolism, small molecule biochemistry	2	1
5	Selenide, water dikinase, **SEPHS1**	–	2	1

a) The focus proteins are indicated with gene names and shown in bold. A score of 2 was considered significant ($p<0.01$).

ubiquitin, which is transferred to a target protein through the action of the E2 variant 1 enzyme. This step of the proteasome machinery seems to be inhibited by reversine treatment.

Beside the degradation *via* proteasome, a differential expression of proteins involved in lysosomal degradation was also observed. This study showed a decrement of vacuolar adenosinetriphosphatase subunit B (−1.68-fold) and an increment of Cathepsin D (+1.79-fold). The latter is a lysosomal aspartic endoprotease, which plays a crucial role in the regulation of apoptosis [48].

3.4 Protein folding

2-D DIGE showed a deregulation (−1.23-fold) of chaperonin containing TCP-1 θ subunit involved in folding, particularly of actin and tubulin both *in vivo* and *in vitro*. Its main function is to bind denaturated/neo-synthetized proteins and to mantain cellular homeostasis [49, 50]. Coghlin *et al.* [51] pointed out that TCP-1 is not only involved in cell growth but is also highly over-expressed in the S-phase of cell cycle.

Additional changes were observed in HSPs whose major role is to assist protein folding. In this study we found that three different HSPs were differentially expressed: HSP9A, 47 kDa HSP (+1.23- and +1.66-fold-change, respectively) and heat shock cognate 71 kDa protein (HSPa8; −1.47-fold change). HSP9A and HSPa8 are members of HSP70 family [52] involved in many biological processes such as stress response, cell death/proliferation and trafficking control [53]. In contrast, tumour rejection antigen gp96, a glycoprotein belonging to HSPs' family, that plays a role in different cellular functions, such as homeostasis and cell proliferation [54], was found decreased (−1.45-fold). Moreover we found an increment of endoplasmic reticulum protein ERp29 precursor (+1.31-fold). This protein participates in protein folding in endoplasmatic reticulum and it plays an important role in the processing of secretory proteins [55].

3.5 Stress control

A strong increment of two cytosolic proteins involved in oxidative stress such as glutathione S-transferase, mu 1

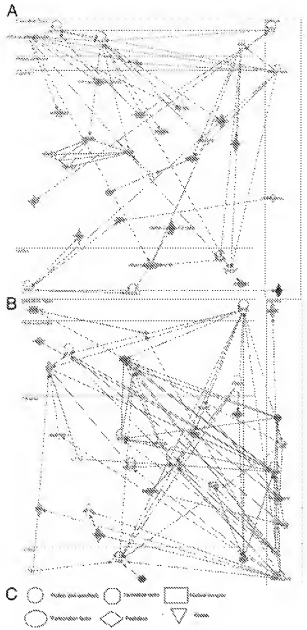

Figure 4. Signaling networks 1 (A) and 2 (B) of murine fibroblast proteins regulated by reversine treatment. Identified differentially changed proteins (indicated by their gene names) were uploaded in IPA. Edges containing single line indicate protein associations, arrows indicate expression-controlling proteins, whereas grey nodes represent the identified proteins (focus proteins). Nodes shapes (C).

(+2.07-fold) and mu 2 (+2.69-fold) subunits was observed. This increment reflects the response to intracellular oxidative stress induced by reversine. Dandrea *et al.* [56] suggested that transient S-glutathionylation of protein is a cross-protection against morphological changes generated by the induction of an oxidative DNA damage and by the presence of agents inducing cell toxicity. Moreover, the most important role of the glutathione *S*-transferase enzymes is the inactivation of xenobiotic agents [57]. Particularly the mu class is active in detoxification of electrophilic compounds, including carcinogens, therapeutic drugs, environmental toxins and products of oxidative stress, by conjugating them with glutathione. Pyrroline-5-carboxylate reductase 1 (+3.96-fold), a proline biosynthetic enzyme, was also up-regulated. Accumulation of proline in cytoplasm is an adaptative response to stress. Krishnan *et al.*, showed that proline influences glutathione levels during H_2O_2 stress treatment [58]. The level of peroxiredoxin 3 was also changed (+1.41-fold). Peroxiredoxins are small proteins often identified in proteomic studies [59], involved in processes such as proliferation, transformation and apoptosis.

Dimethylarginine dimethylaminohydrolase 2 which hydrolyzes N(G),N(G)-dimethyl-L-arginine and N(G)-monomethyl-L-arginine acting as a NOS inhibitor and playing a role in nitric oxide generation was also slightly increased (+1.15-fold), whereas the selenophosphate synthetase 1 was slightly decreased (−1.13-fold). This protein is involved in ATP binding and selenocysteine synthesis [60]. In addition, glutamate dehydrogenase 1 mitochondrial precursor, which is a reducing enzyme involved in energy storage, was found increased (1.41-fold).

3.6 Metabolism

Phosphoenol pyruvate carboxy kinase 2, involved in gluconeogenesis and nucleotide binding, and fructose-bisphosphate aldolase catalyzing the reversible conversion of Fru-1,6-biphosphate to glyceraldehyde 3-phosphate and dihydroxy-acetone were more abundant (+2.03- and +3.55-fold, respectively) in reversine treated cells. Both enzymes, however, are gluconeogenic intermediates and elevate the intracellular levels of ATP [61, 62] supporting energy demand. In contrast the conversion of glyceraldehyde 3-phosphate to dihydroxy-acetone phosphate was reduced due to a decrement of triosephosphate isomerase (−1.54-fold). Adenylate kinase 1, a small ubiquitous enzyme that is essential for maintenance and cell growth, and the mitochondrial serine hydroxymethyltransferase 2, which regulates the inter-conversion of serine and glycine to generate pyruvate, were increased (+1.58- and +1.63-fold, respectively).

Five enzymes related to mitochondrial activity were also more abundant: Acyl-CoA thioesterase 2, the long chain-specific Acyl CoA dehydrogenase, the electron transfer flavoprotein subunit α, enoyl CoA hydratase and NADH dehydrogenase (ubiquinone) 1 α subcomplex 10 (+2.35, + 1.69, +2.7, +1.53 and +1.63, respectively), suggesting an activation of the aerobic metabolism. The acyl-CoA thioesterases are a group of enzymes that catalyze the hydrolysis of acyl-CoA to free fatty acid and coenzyme A (CoASH) by interacting with long chain-specific acyl-CoA dehydrogenase, providing the potential to regulate intracellular

levels of acyl-CoA, free fatty acids and CoASH. The third enzyme acts as a specific electron acceptor of dehydrogenases, including five acyl-CoA dehydrogenases transferring electrons to the main mitochondrial respiratory chain *via* electron transfer to ubiquinone oxidoreductase. Enoyl-CoA hydratase is involved in the second step of β-oxidation of fatty acids by catalyzing the reversible hydration of trans-2-enoyl-CoA thioesters to the corresponding 3-hydroxyacyl-CoA thioesters [63], whereas NADH dehydrogenase (ubiquinone) 1 α subcomplex 10, is a key enzyme of the respiratory chain complex 1.

confirmed by our analysis (+2.14-fold). The mammalian cytochrome P450 is a component of membrane-bound monooxygenase family involved in xenobiotic agents, drug metabolism and signalling of endogenous molecules [65]. This family of enzymes can be regulated by a number of post-translational events *in vivo*, including availability of catalytic treatment, post-translational modifications and protein–protein

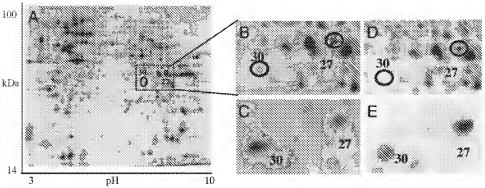

Figure 5. 2-D DIGE of control sample (Cy5 labelled) (A) and close-up of the 45 kDa region containing annexin A3 (spots 27 and 30 in Table 1) (B), annexin A3 identification by monoclonal antibody after electrotransfer to PVDF membrane (C), annexin A3 localization in reversine-treated sample (D) and after antibody recognition (E). Proteins were separated in a NL pH 3–10 IPG strip in the first dimension and SDS gel (12% T, 2.5% C) in the second and electrotransferred onto PVDF membranes. The membranes were incubated with monoclonal anti-annexin A3 (1:30 000 as primary antibody) and HRP conjugate anti-mouse (1:70 000 as secondary antibody). Proteins were visualized by chemiluminescence using ECL Advance kit.

3.7 Others

Among the more abundant proteins we can indicate annexins (A3, A5 and A7) and calreticulin. The latter is a multifunctional protein involved, as annexin, in Ca^{2+} binding and folding [64] and was +1.17-fold increased.

Annexins 3 and 5 were identified with different isoforms in a 2-D map, whereas annexin 7 was present as a single increased spot (+1.63). These cytosolic proteins are involved in binding of Ca^{2+} enabling the interaction with membrane phospholipids, and in membrane-binding regulating cell signaling and proliferation. Both isoforms of annexins A5 were more abundant in reversine-treated fibroblasts (+1.13- and +1.46), whereas annexins A3 showed a differential trend of the two isoforms: annexin 3 corresponding to spot 30 was decreased (−1.36), whereas isoform of spot 27 was increased (+1.39). Furthermore, the representative 2-D map indicates both annexins A3 have a more alkaline isoelectric point in comparison with the theoretical one suggesting the possible presence of a post-translational modification, the investigation of which is out of the topic.

Previous proteomic investigations on myoblasts [6], indicating an increment of cytochrome P450 after 1- 6 reversine treatment (family 19, subfamily a, polypeptide 1) were

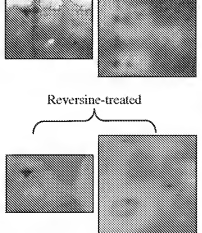

Figure 6. Close-up of a 2-D gel for the assessment of protein ubiquitination after immunoblotting of 100 μg protein extract from control and reversine-treated fibroblasts. Proteins were separated in a NL pH 3–10 IPG strip in the first dimension and SDS gel (12% T, 2.5% C) in the second and electrotransferred onto PVDF membranes. The membranes were incubated with antibodies diluted in the following way: monoclonal anti-ubiquitin (1:20 000 as primary antibody) and HRP conjugate anti-mouse (1:50 000 as secondary antibody). Proteins were visualized by chemiluminescence using the ECL Advance kit.

interactions [66, 67]. Particularly, P450 19A1 has been related to breast cancer due to its involvement in estrogens biosynthesis. The enhanced expression of P450 19A1 actually increases estrogen production, resulting in a positive feedback loop to drive hormone-responsive breast cancer cell growth [68]. In our cellular model we can speculate on the positive role of this overexpression. Estrogens and their receptors, play a role in regulating processes related to start, progression and exit from the G1 phase of the cell cycle [69, 70].

Mtr3 (mRNA transport regulator 3)-homolog, a component of the exosome 3′–> 5′ exoribonuclease complex degrading unstable mRNAs and containing AU-rich elements required for the 3′-processing of the 7S pre-RNA to the mature 5.8S rRNA, was increased (+1.64-fold).

Another protein involved in m-RNA processing was found deregulated: the heterogeneous nuclear ribonucleoprotein A2/B1 isoform 2 (−1.16). This protein is involved in pre-mRNA processing and its change is a signal (together with ubiquitin-conjugating enzyme E2 decrease) of DNA damage and transcription detuning [71]. DEAD (Asp-Glu-Ala-Asp) box polypeptide 39, involved in pre-mRNA splicing and required for the export of mRNAs out of the nucleus, was decreased (−1.45-fold). The deregulation of these two proteins suggests a direct modulation of reversine both in the elimination of the elements, which could induce instability, and in the control of the nuclear mRNA export.

Finally we found a variation concerning interleukin-25 (+1.41-fold), which is involved in immunity response by modulating cytokines expression, such as IL-5 and IL-13; however, its regulatory function remains unknown [72].

3.8 Validation

With regard to differential expression of annexin 3 isoforms and their localization on the 2-D map, blotting was conducted after separation on 24 cm pH 3–10 NL gradient. Figure 5 shows the results of detection of the two isoforms in a control and reversine-treated samples. Spots are differentially abundant in controls *versus* reversine-treated fibroblasts according to DeCyder quantitation trend. In addition, both isoforms were recognized suggesting that changes in apparent molecular weight and *pI* could be a result of a post-translational modification, which will be characterized in further studies.

As to annexin 3, ubiquitinated proteins were also analysed by immunoblotting after 2-DE separation under the same gradient and electrophoretic conditions. The number and the amount of ubiquitinated proteins were lower after reversine treatment, supporting the 2-D-DIGE information. Figure 6 shows a close-up of ubiquitinated proteins identified by immunoblotting on control and treated sample.

A further validation of our differential results was obtained by quantifying lamin A/C expression and locali-

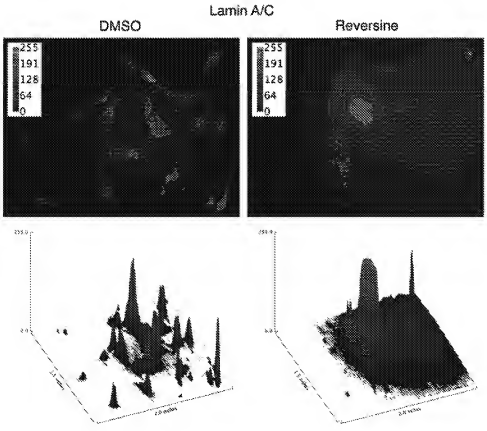

Figure 7. Assessment of lamin A/C increase after reversine treatment. Immunofluorescence staining of murine fibroblasts with antibody against lamin A/C (red) performed after 72 h of DMSO (left panels) or 5 μM reversine treatment (right panels). Fluorescence microscopy (20×) reveals higher levels of lamin A/C staining in reversine-treated cells, as shown in the surface plot analysis (lower panels). Fluorescence intensity scale is also reported in the inset graphs.

zation by immunofluorescence as shown in Fig. 7. The results are in agreement with the proteomic differential analysis.

4 Concluding remarks

Induced stem cells could be a valid source in addition to adult and embryonic stem cells in order to obtain the widest extensions, in terms of different organs and tissues to be replaced in regenerative medicine. The use of "small molecules" to produce induced stem cells is being adopted by an increasing number of research groups. Therefore, it has become crucial to understand the mechanisms underlying the de-differentiation process. This would allow finding the ways to increase the efficiency of the process, and to assess its safety. In particular, a wide-range proteomic investigation coupled with advanced bioinformatic tools seems a powerful approach to study the effects induced by de-differentiating drugs such as reversine. Although the raw data output from a comprehensive proteomic analysis may result quite difficult to be interpreted, the use of bioinformatic algorithms, as the IPA software, may give important hints to recognize or predict the major cell pathways affected by reversine treatment. In fact, as shown in this study, reversine appears to exert a crucial role on specific proteins involved in cell cycle arrest, cytoskeletal remodelling, stress response, mRNA export, cell signalling and proliferation. These protein changes, as anticipated, will require further studies to be validated, but constitute an important step-forward towards the understanding of reversine mechanism of action.

This work has been funded from: Italian Ministry of University and Scientific Research (Grant: FIRB RBRNO7BMCT to C.G.)

The authors have declared no conflict of interest.

5 References

[1] Takahashi, K., Yamanaka, S., *Cell* 2006, *126*, 663–676.

[2] Ding, S., Schultz, P. G., *Nat. Biotechnol.* 2004, *22*, 833–840.

[3] Chen, S., Zhang, Q., Wu, X., Schultz, P. G., Ding, S., *J. Am. Chem. Soc.* 2004, *126*, 410–411.

[4] Anastasia, L., Sampaolesi, M., Papini, N., Oleari, D., Lamorte, G., Tringali, C., Monti, E. *et al.*, *Cell Death Differ.* 2006, *13*, 2042–2051.

[5] Chen, S., Takanashi, S., Zhang, Q., Xiong, W., Zhu, S., Peters, E.C., Ding, S. *et al.*, *Proc. Natl. Acad. Sci. USA* 2007, *104*, 10482–10487.

[6] Shan, S. W., Tang, M. K., Chow, P. H., Maroto, M., *Cai, D. Q., Lee, K. K., Proteomics 2007, 7, 4303–4316.*

[7] D'Alise, A. M., Amabile, G., Iovino, M., Di Giorgio, F. P., Bartiromo, M., Sessa, F., Villa, F. *et al.*, *Mol. Cancer Ther.* 2008, *7*, 1140–1149.

[8] Hsieh, T. C., Traganos, F., Darzynkiewicz, Z., Wu, J. M., *Int. J. Oncol.* 2007, *31*, 1293–1300.

[9] Kim, Y. K., Choi, H. Y., Kim, N. H., Lee, W., Seo, D.W., Kang, D. W., Lee, H. Y. *et al.*, *Biochem. Biophys. Res. Commun.* 2007, *358*, 553–558.

[10] Li, R., Zhu, S., He, X., Xie, Z., *Cell Biol. Int.* 2007, *31*, 540–545.

[11] Perreira, M., Jiang, J. K., Klutz, A. M., Gao, Z. G., Shainberg, A., Lu, C., Thomas, C. J. *et al.*, *J. Med. Chem.* 2005, *48*, 4910–4918.

[12] Karp, N. A., Lilley, K. S., *Proteomics* 2005, *5*, 3105–3115.

[13] Marouga, R., David, S., Hawkins, E., *Anal. Bioanal. Chem.* 2005, *382*, 669–678.

[14] Karp, N. A., Kreil, D. P., Lilley, K. S., *Proteomics* 2004, *4*, 1421–1432.

[15] Tonge, R., Shaw, J., Middleton, B., Rowlinson, R., Rayner, S., Young, J., Pognan, F. *et al.*, *Proteomics* 2001, *1*, 377–396.

[16] Zhou, G., Li, H., DeCamp, D., Chen, S., Shu, H., Gong, Y., Flaig, M. *et al.*, *Mol. Cell. Proteomics* 2002, *1*, 117–124.

[17] Ji, H., Erfani, N., Tauro, B. J., Kapp, E. A., Zhu, H. J., Moritz, R. L., Lim, J. W. *et al.*, *Electrophoresis* 2008, *29*, 2660–2671.

[18] Moriggi, M., Cassano, P., Vasso, M., Capitanio, D., Fania, C. , Musicco, C., Pesce, V. *et al.*, *Proteomics* 2008, *8*, 3588–3604.

[19] De Palma, S., Ripamonti, M., Vigano, A., Moriggi, M., Capitanio, D., Samaja, M., Milano, G. *et al.*, *J. Proteome Res.* 2007, *6*, 1974–1984.

[20] Danieli Betto, D., Zerbato, E., Betto, R., *Biochem. Biophys. Res. Commun.* 1986, *138*, 981–987.

[21] Righetti, P. G., Gelfi, C., *J. Biochem. Biophys. Methods* 1984, *9*, 103–119.

[22] Feng, Y., Walsh, C. A., *Nat. Cell Biol.* 2004, *6*, 1034–1038.

[23] Ohta, Y., Hartwig, J. H., Stossel, T. P., *Nat. Cell Biol.* 2006, *8*, 803–814.

[24] Stossel, T. P., Condeelis, J., Cooley, L., Hartwig, J. H., Noegel, A., Schleicher, M., Shapiro, S. S., *Nat. Rev. Mol. Cell. Biol.* 2001, *2*, 138–145.

[25] Meng, X., Yuan, Y., Maestas, A., Shen, Z., *J. Biol. Chem.* 2004, *279*, 6098–6105.

[26] Ohta, Y., Kousaka, K., Nagata-Ohashi, K., Ohashi, K., Muramoto, A., Shima, Y., Niwa, R. *et al.*, *Genes Cells* 2003, *8*, 811–824.

[27] Lappalainen, P., Drubin, D. G., *Nature* 1997, *388*, 78–82.

[28] Hosoda, A., Sato, N., Nagaoka, R., Abe, H., Obinata, T., *J. Muscle Res. Cell Motil.* 2007, *28*, 183–194.

[29] Larsen, A. K., Lametsch, R., Elce, J., Larsen, J. K., Thomsen, B., Larsen, M. R., Lawson, M. A. *et al.*, *Biochem J* 2008, *411*, 657–666.

[30] Oakley, B. R., *Trends Cell Biol.* 2000, *10*, 537–542.

[31] Bennett, M. R., Ravipati, N., Ross, G., Nguyen, M. T., Hirsch, R., Beekman, R. H., Rovner, L. *et al.*, *Proteomics Clin. Appl.* 2008, *2*, 1058–1064.

[32] Mills, J. C., Stone, N. L., Erhardt, J., Pittman, R. N., *J. Cell Biol.* 1998, *140*, 627–636.

[33] Lemasters, J. J., DiGuiseppi, J., Nieminen, A. L., Herman, B., *Nature* 1987, *325*, 78–81.

[34] DesMarais, V., Ghosh, M., Eddy, R., Condeelis, J., *J. Cell Sci.* 2005, *118*, 19–26.

[35] Ghosh, M., Song, X., Mouneimne, G., Sidani, M., Lawrence, D. S., Condeelis, J. S., *Science* 2004, *304*, 743–746.

[36] Vydra, J., Selicharova, I., Smutna, K., Sanda, M., Matousková, E., Bursíková, E., Prchalová, M. *et al.*, *BMC Cancer* 2008, *8*, 107.

[37] Amin, M. A., Matsunaga, S., Uchiyama, S., Fukui, K., *Biochem. J.* 2008, *415*, 345–351.

[38] Maggi, L. B., Jr., Kuchenruether, M., Dadey, D. Y., Schwope, R. M., Grisendi, S., Townsend, R. R., Pandolfi, P. P. *et al.*, *Mol. Cell. Biol.* 2008, *28*, 7050–7065.

[39] Tuynder, M., Fiucci, G., Prieur, S., Lespagnol, A., Géant, A., Beaucourt, S., Duflaut, D. *et al.*, *Proc. Natl. Acad. Sci. USA* 2004, *101*, 15364–15369.

[40] Schirmer, E. C., Gerace, L., *Trends Biochem. Sci.* 2005, *30*, 551–558.

[41] Worman, H. J., Courvalin, J. C., *J. Clin. Invest.* 2004, *113*, 349–351.

[42] Lee, J. S., Hale, C. M., Panorchan, P., Khatau, S. B., George, J. P., Tseng, Y., Stewart, C. L. *et al.*, *Biophys. J.* 2007, *93*, 2542–2552.

[43] Song, X., von Kampen, J., Slaughter, C. A., DeMartino, G. N. *J. Biol. Chem.* 1997, *272*, 27994–28000.

[44] Kuehn, L., Dahlmann, B., *Mol. Biol. Rep.* 1997, *24*, 89–93.

[45] Adams, J., *Cancer Treat Rev.* 2003, *29*, 3–9.

[46] Shah, S. A., Potter, M. W., McDade, T. P., Ricciardi, R., Perugini, R. A., Elliott, P. J., Adams, J. *et al.*, *J. Cell. Biochem.* 2001, *82*, 110–122.

[47] Teicher, B. A., Ara, G., Herbst, R., Palombella, V. J., Adams, J., *Clin. Cancer Res.* 1999, *5*, 2638–2645.

[48] Roberg, K., Kagedal, K., Ollinger, K., *Am. J. Pathol.* 2002, *161*, 89–96.

[49] Dekker, C., Stirling, P. C., McCormack, E. A., Filmore, H., Paul, A., Brost, R. L., Costanzo, M. *et al.*, *EMBO J.* 2008, *27*, 1827–1839.

[50] Hynes, G., Sutton, C. W., U, S., Willison, K. R., *FASEB J.* 1996, *10*, 137–147.

[51] Coghlin, C., Carpenter, B., Dundas, S. R., Lawrie, L. C., Telfer, C., Murray, G. I., *J. Pathol.* 2006, *210*, 351–357.

[52] McHugh, P. C., Rogers, G. R., Loudon, B., Glubb, D. M., Joyce, P. R., Kennedy, M. A., *J. Neurosci. Res.* 2008, *86*, 306–316.

[53] Wadhwa, R., Taira, K., Kaul, S. C., *Cell Stress Chaperones* 2002, *7*, 309–316.

[54] Glen, A., Gan, C. S., Hamdy, F. C., Eaton, C. L., Cross, S. S., Catto, J. W., Wright, P. C. *et al.*, *J. Proteome Res.* 2008, *7*, 897–907.

[55] Mkrtchian, S., Fang, C., Hellman, U., Ingelman-Sundberg, M., *Eur. J. Biochem.* 1998, *251*, 304–313.

[56] Dandrea, T., Bajak, E., Warngard, L., Cotgreave, I. A., *Arch. Biochem. Biophys.* 2002, *06*, 241–252.

[57] Bostwick, D. G., Meiers, I., Shanks, J. H., *Hum. Pathol.* 2007, *38*, 1394–1401.

[58] Krishnan, N., Dickman, M. B., Becker, D. F., *Free Radic. Biol. Med.* 2008, *44*, 671–681.

[59] Petrak, J., Ivanek, R., Toman, O., Cmejla, R., Cmejlova, J., Vyoral, D., Zivny, J. *et al.*, *Proteomics* 2008, *8*, 1744–1749.

[60] Xu, X. M., Carlson, B. A., Mix, H., Zhang, Y., Saira, K., Glass, R. S., Berry, M. J. *et al.*, *PLoS Biol.* 2007, *5*, e4.

[61] Kraus-Friedmann, N., Feng, L., *Metabolism* 1996, *45*, 389–403.

[62] Yanez, A. J., Ludwig, H. C., Bertinat, R., Spichiger, C., Gatica, R., Berlien, G., Leon, O. *et al.*, *J. Cell. Physiol.* 2005, *202*, 743–753.

[63] Agnihotri, G., Liu, H. W., *Bioorg. Med. Chem.* 2003, *11*, 9–20.

[64] Alfonso, P., Nunez, A., Madoz-Gurpide, J., Lombardia, L., Sanchez, L., Casal, J. I., *Proteomics* 2005, *5*, 2602–2611.

[65] Wright, A. T., Cravatt, B. F., *Chem. Biol.* 2007, *14*, 1043–1051.

[66] Aguiar, M., Masse, R., Gibbs, B. F., *Drug Metab. Rev.* 2005, *37*, 379–404.

[67] Oesch-Bartlomowicz, B., Oesch, F., *Arch. Toxicol.* 1990, *64*, 257–261.

[68] Miller, T. W., Shin, I., Kagawa, N., Evans, D. B., Waterman, M. R., Arteaga, C. L., *J. Steroid Biochem. Mol. Biol.* 2008, *112*, 95–101.

[69] Doisneau-Sixou, S. F., Sergio, C. M., Carroll, J. S., Hui, R., Musgrove, E. A., Sutherland, R. L., *Endocr. Relat. Cancer* 2003, *10*, 179–186.

[70] Foster, J. S., Henley, D. C., Ahamed, S., Wimalasena, J., *Trends Endocrinol. Metab.* 2001, *12*, 320–327.

[71] Yang, S., Liu, T., Li, S., Zhang, X., Ding, Q., Que, H., Yan, X., *Neuroscience* 2008, *154*, 1107–1120.

[72] Tato, C. M., Laurence, A., O'Shea, J. J., *J. Exp. Med.* 2006, *203*, 809–812.

